DOI: 10.1002/ ((please add manuscript number))
Article type: Article

Portable molecularly imprinted polymer-based platform for detection of histamine in aqueous solutions

*Shishir Venkatesh,[1,2], Chi-Chung Yeung[2,3], Tan Li[1], Siu Chuen Lau[1,2], Qi-Jun Sun[1], Ling-Yi Li[4], Jin Hua Li[5], Michael H. W. Lam[3], Vellaisamy A. L. Roy[6 *]*

[1] State Key Laboratory for Millimeter Waves and Department of Material Science & Engineering, City University of Hong Kong, 83 Tat Chee Avenue, Kowloon, Hong Kong S. A. R.
[2] Portalyze Point of Care Limited, Hong Kong Science and Technology Park, Pak Shek Kok, Hong Kong S.A.R.
[3] Department of Chemistry, City University of Hong Kong, 83 Tat Chee Avenue, Kowloon, Hong Kong, S. A. R.
[4] Xiamen Innov Information Technology Co. Ltd., Xiamen, Fujian, P. R. China
[5] Fisheries College, Jimei University, Xiamen, Fujian, P. R. China
[6] James Watt School of Engineering, University of Glasgow, G12 8QQ, United Kingdom

Email: Roy.Vellaisamy@glasgow.ac.uk (Dr. Vellaisamy A. L. Roy)

Keywords: flexible histamine sensor, seafood contamination, portable smartphone-based sensor

ABSTRACT

Histamine, which is a naturally occurring chemical in seafood, is known to cause undesirable inflammatory response when consumed in large amounts. Histamine is produced in unsafe amounts in colored seafood when improperly stored for just a few hours. Food and health regulatory bodies across the world have guidelines limiting the amount of histamine in fresh as well as processed seafood. Conventional histamine detection is performed in testing labs, which is a slow process and results in bottlenecks in the seafood supply-chain system. A system to rapidly detect the seafood histamine levels on site is very desirable for seafood suppliers. Herein, we describe an impedance-based histamine detection sensor built on a flexible substrate that can detect histamine in the range of 100-500 ppm. Moreover, our sensor discriminates histamine in the

presence of DL-histidine and other biogenic amines, with the selectivity provided by molecular imprinting technology. As a proof of concept, a smartphone controlled, portable semi-quantitative histamine sensing device was fabricated that gave out reliable testing results for histamine in different test solutions as well as for real seafood. We believe this technology can be extended towards determination of other food contaminants in aqueous solutions.

1. Introduction

Histamine is an important biological chemical involved in the immunological response to pathogens in humans(Stein et al., 1976; Delves and Roitt, 2000; Jutel et al., 2005). Most of the histamine in humans is generated by immunological mast cells(Johnson and Erdös, 1973; Hallgren and Gurish, 2014) and basophils(Belon et al., 2004) through the enzyme-assisted decarboxylation of the histidine amino-acid(Eitenmiller et al., 1981). Additionally, histamine can also come from dietary sources such as fermented and spoiling foods such as fish, cheese and wines(Ijomah et al., 1991). Overexposure from dietary sources results in elevated bodily histamine which in turn is responsible for syndromes like histamine intolerance(Taylor, 1985; Maintz and Novak, 2007) and histamine poisoning(Schirone et al., 2017). The maximum legal limits in the European Union under Regulation No. 1441/2007 for histamine for different species of fish like *Scombridae*, *Clupeidae*, *Engraulidae*, *Coryfenidae*, *Pomaomidae* and *Scombresosidae* range from 100 – 400 ppm(Commission Regulation, 2007). As such, seafood suppliers across the globe now have to send samples to testing labs as part of the HACCP quality control procedures. However, this is a slow process and causes bottlenecks in the seafood supply-chain system. Therefore, a simple & rapid system to determine the concentration of histamine on-site is desired by seafood suppliers.

Conventional methods of histamine detection in food use laboratory based techniques such as separation using solid phase extraction followed by high performance liquid

chromatography(Busto et al., 1994; Önal, 2007; Tahmouzi et al., 2011; Tang et al., 2011; Dang et al., 2013, Mohammed et al., 2016, Liu et al., 2018) and ELISA assays in conjunction with fluorescent tags(Marcobal et al., 2005; Köse et al., 2011). The former technique requires extensive sample preparation, large laboratory equipment while the latter uses expensive testing kits, optical components and storage under refrigerated conditions(Bedia Erim, 2013). Also, both these techniques are not really suitable for rapid on-site analysis of histamine. Colorimetric methods, such as AOAC 977.13 and GB 5009.208, for the determination of histamine have been developed(Staruskiewicz, 1977). However, these methods require complex and time consuming extraction procedures making it difficult to employ for on-site detection by a non-trained user. Lateral flow assays for histamine detection are also colorimetric but they use biological receptors such as enzymes and antibodies which make them expensive and require storage under refrigeration. Alternative colorimetric methods require labelling the sample with quantum dots(Shi et al., 2020), Au nanoparticles(Bi et al., 2020), and azo-based compounds(Lv et al., 2019), which again is not feasible for most on-site testing. Electrochemical sensing is an alternative method that can be used in on-site label-free analysis of histamine. Electrochemical methods include voltammetry(Henao-Escobar et al., 2015; Akhoundian et al., 2017; Kumar and Goyal, 2018), potentiometry(Basozabal et al., 2014) and impedance spectroscopy(Bongaers et al., 2010; Horemans et al., 2010; Delle et al., 2015). Potentiometry and voltammetry rely on the development of charge and current signal upon analyte-receptor binding event. This usually requires the analyte to be electrochemically active. Impedance spectroscopy on the other hand is a technique to characterize the kinetics of an electrochemical system and is used in the determination of the concentration of an analyte not involved in redox processes. Moreover, the AC voltage applied to the active layers in impedance spectroscopy prevents electrode polarization and fouling. In

impedance spectroscopy, the signal parameter measured, is ΔZ (magnitude and phase) of an active sensor layer.

Usually the component that forms the active layer for an impedimetric sensor is the receptor layer. The function of the receptor layer is to selectively bind with the analyte of interest. Previous studies have used enzymes(Zeng et al., 2000; Bao et al., 2002; Henao-Escobar et al., 2016; Papageorgiou et al., 2018), aptamers(Hasanzadeh et al., 2017), molecularly imprinted polymer(Rotariu et al., 2016) and self-assembly monolayers(Minamiki et al., 2015) as receptors in electrochemical histamine sensors. Among these receptors, molecularly imprinted polymers (MIPs) are the most stable and robust, while offering specific recognition properties, making them suitable for on-site analysis. MIPs have been used as the receptor layer in biosensors with optical(Liu et al., 2020) as well as electrochemical(Qi et al., 2019) transduction mechanisms for biological and environmental applications. MIPs are synthesized via polymerization of a functional monomer in the presence of the template (analyte). Removal of the template after polymerization, leaves voids in the polymer matrix that where specific interaction can take place with the analyte of interest(Chen et al., 2016, Yoshikawa et al., 2016). As mentioned previously, the MIP forms the active layer in an impedimetric device. Specific interactions with the template (analyte) molecule in this layer causes the impedance of this layer to change.

Additional sensor characteristics that need to be considered are large-scale manufacturability, cost of a single sensor head and easy operation. The widespread proliferation of smartphones in our society has made it an attractive platform, from which sensors can be operated with simplicity. There are literature reports of smartphone-controlled sensors for portable environmental sensing applications(Wang et al., 2020). Herein, we show a flexible histamine sensing device (for histamine detection in aqueous media) based on impedance spectroscopy and

MIPs. The sensor is fabricated on a large scale using readily available and cheap materials. The results show excellent selectivity towards histamine and the detection range is within the relevant range with regards to regulatory limits. Finally, this sensor head is applied towards a semi-quantitative on-site testing device which is controlled via a smartphone app. Based on the promising results of this portable platform, we believe this histamine detection system can be simply repurposed and targeted towards other food contaminants.

2. Material and Methods

2.1 Modelling and simulation

MD simulations were performed in GROMACS(Abraham et al., 2015). The simulations employed the GROMACS 54a7 force field(Huang et al., 2011). The model system consists of methacrylic acid (monomer) molecules and histamine (receptor) molecules in different stoichiometry ratios (number of histamine molecules is fixed at 100 for all simulation trials), in a cubic box of 50 Angstrom with periodic boundary conditions at temperature 298 K. The corresponding molecular topologies and force file parameters are downloadable from the Automated Topology Builder (ATB) and Repository(Malde et al., 2011).

Randomized initially packing geometries are used and are constructed by Packmol package(Martínez et al., 2009). The MD simulations of pure components molecules were carried out starting from random orientations and Gaussian distribution velocities. After a series of energy minimization steps and equilibration, the production runs were carried out in the NVT ensemble(Titantah and Karttunen, 2013).

Study of the interactions of the component molecules in different stoichiometric mixture is performed by examining the trajectories of all the components in the system over the NVT

ensemble, using hydrogen bond analyses. Average hydrogen bond number was calculated by averaging the number of hydrogen bond over the trajectory and over all molecules (histamine to histamine H-bond, methacrylic acid to methacrylic acid H-bond, and histamine to methacrylic acid H-bond). A detailed analysis of the hydrogen bonding in the mixtures was performed and the results are shown in **Figure 1**.

2.2 Materials

Metharcylic acid, ethylene glycol dimethacrylate, histamine, ammonium persulfate, acetic acid (99%) and tetramethylethylenediamine (TEMED) were purchased from Sigma-Aldrich, USA and used without further purification. Dimethyl sulfoxide (DMSO) and methanol – ACS reagent grade solvents are purchased from Oriental Chemicals, Hong Kong and used without further purification.

2.3 Synthesis of MIP

A mixture of 2 mmol methacrylic acid monomer (MAA), 10 mmol ethylene glycol dimethacrylate cross-linker (EGDMA) are dissolved in 10 mL dimethylsulphoxide (DMSO) together with the 1mmol histamine template in a 100 mL round bottom flask. The mixture is stored in a dark place for 6hrs. Then, 0.01 mmol ammonium persulfate is added into the mixture, and the mixture is degassed by pumping nitrogen gas for 30mins. 5 µmol of tetramethylethylenediamine initiator is added into the mixture solution to trigger the polymerization. After 24hrs polymerization, the resulting bulk polymer is washed with methanol roughly, ground and transferred into a thimble. Subsequently, the template is removed from the MIP powders by consecutive the Soxhlet extraction, starting with a mixture of acetic acid/ methanol (1:1) (48 h), followed by methanol (24 h) and finally with acetone (12 h). The resulting MIP powder is dried in vacuum for 12 h. Subsequently, the powder is further grounded and sieved through a 50 µm mesh.

The corresponding non-imprinted polymer (NIP) was prepared using the same procedure but without the addition of the histamine template.

2.4 Fabrication of sensor

The sensor uses a two –interdigitated electrode design as described in **Figure 1c**. 18 µm thick Copper on polyimide substrates are purchased. The interdigitated copper electrodes were patterned via a photolithography and wet-etching (Iron (III) chloride) process. The spacing between the two interdigitated electrodes is maintained at 40 µm. Subsequently, the interdigitated electrodes are coated with a 6 µm thick polyurethane (PU) adhesive film. To fix the MIP micro particles into PU film, the sensor is placed on a hot plate set to 130°C, which is beyond the glass transition temperature of the 6 µm PU film. MIP particles are embedded into this soft polymer layer and the sensor head is slowly cooled down to room temperature.

2.5 Sensor characterization

Impedance spectroscopy is carried out across the interdigitated electrodes as shown in **Figure 2a**. The impedance response of the flexible histamine response was measured using a CHI660E, CHI instruments USA, in potentiometric mode. The frequency was swept from 100 kHz to 100 Hz, with a 100 mV (peak-peak) sine wave. Standard solutions of histamine were prepared by serial dilution in deionized water.

2.6 Real seafood sample preparation

Two shrimp (*White Shrimp*) and two fish samples (*Grass Carp*) were purchased from a local supermarket for demonstration of smartphone-controlled portable device. One fish and one shrimp were stored in a 4°C refrigerator for 24 hours while the other two samples were stored in a

25°C fume-cupboard for 48 hours. Section 2.6.1 and 2.6.2 briefly explain the sample preparation procedures for the portable MIP-based histamine sensor & for HPLC-MS respectively.

2.6.1 For portable MIP-based histamine sensor

Cut the seafood into 1 g pieces and place in a glass vial. Add 1mL DI water to the vial and mix thoroughly with a spatula. Sample is ready for testing with portable MIP-based histamine sensor.

2.6.2. Histamine extraction procedure for HPLC-MS analysis

Seafood samples were cut into 10 g pieces placed in a glass vial. 50 mL of 0.1 M HCl and 0.1 mL 1000 mg•mL^{-1} of internal standard (1,8-diaminooctane) was added. After thorough mixing with a vortexer, the mixture is filtered through a 0.2 µm nylon filter. The sample is ready for analysis by HPLC-MS. HPLC-MS analysis was performed in accordance with Agilent documentation no. 5991-1286EN .

3. Results and Discussion

3.1 Computer simulation results

In **Figure 1d** that the efficacy of methacrylic acid to histamine H-bond formation approximately reaches an inflection point when of number of acid molecules increases beyond 200. The inflection point at ca. 200 represents a formation of optimal methacrylic acid to histamine H-bond network that insertion of the of extra methacrylic acid molecules into this network becomes less favourable beyond this point. As shown in **Figure 1c,** the histamine molecule contains 2 nitrogen atoms (shown in blue) with one lone pair of electrons each available for H-bond formation. These lone pair of electrons form H-bond with carboxylic acid group from 2 different methacrylic acid molecules. The lone pair of the third nitrogen atom in histamine is delocalized in the π-orbital of the 5-member ring of histamine. From these results, it can be inferred

that molar ratio of 2:1 methacrylic acid: histamine is the optimum ratio for the pre-polymer mixture.

3.2 MIP characterization and confirming its immobilization on the surface of the sensor

The SEM image of the MIP micro-particle is presented in **Figure 3a**. The particle size is around 10 µm. The morphology is irregular with the irregularity having been caused by the grinding process. **Figure 3b**, **c** are optical microscope images of the interdigitated electrodes functionalized with the MIP. The images confirm successful immobilization of MIP on the 6 µm PI film in the channel between the electrodes and with good coverage.

3.3 Modelling of the histamine sensor response with an equivalent circuit

In impedance spectroscopy, it is of paramount important to model the impedance behavior with the help of an equivalent circuit. First, the sensor is tested with 500 ppm of histamine in deionized water (pH = 6.8). The response is modeled with a suitable equivalent circuit. As shown in Figure 3a, the Nyquist plot in **Figure 4a** matches well with the simulated data from equivalent circuit used in **Figure 4b**. The equivalent circuit consists of ***Rs*** which is the solution resistance, ***CPE*** which is the constant phase element or an "imperfect capacitor" at the MIP/sample interface and the ***Rct*** which represents the charge-transfer resistance. Histamine at neutral pH solutions retains a positive charge on its amine group. When this charged molecule selectively binds with the MIP, it denotes as a charge transfer from the sample to the sensor surface.

3.4 Characterization of sensor response

We tested the impedance response of the sensor to various concentrations of histamine diluted in deionized water. As shown in **Figure 5a**, there is general decreasing impedance as the concentration of histamine increases. In order to understand the mechanism, the equivalent circuit is modeled. For this equivalent circuit, the ***Rct*** is extracted. As shown, in **Figure 5c**, the ***Rct***

decreases as the concentration of histamine increases. The main interaction between histamine and methacrylic acid in aqueous medium is in the form of ionic bonds(Trikka et al., 2012). So, as number of ionic bonds increase with the increase in concentration of histamine, the charge transfer resistance decreases. In an effort to simulate practical situation, we also tested the flexible histamine sensor for different concentrations of histamine with a constant histidine background of 1000 ppm. The results are presented in **Figure 5b**. The calibration curves are presented as a function of charge transfer resistance in response to the varying concentration of histamine in 2 background solutions: deionized water and 1000 ppm histidine is shown in **Figure 5c**. The two curves are in good agreement expect for the 0 ppm point. In deionized, the lack of ions in the solution results in a very high charge transfer resistance. DL-histidine in water is a polar charged amino acid molecule and can interact non-specifically with the MIP to produce a lower charge transfer resistance. However, upon the addition of histamine, both curves follow the same trend and produce similar values. Therefore, such a device can be used to detect histamine in practical situations where there is a high background concentration of histidine amino acids. However, for on-site testing, it is not very convenient to extract the ***Rct*** data from impedance spectroscopy. It is much simpler to "read-out" the absolute value of impedance ($\boldsymbol{Z_{abs}}$) at a particular frequency. Therefore, we record the $\boldsymbol{Z_{abs}}$ at 4000 Hz. As shown in **Figure 5d**, a ~65% change in $\boldsymbol{Z_{abs}}$ is observed as the concentration of histamine increases from 0 to 100 ppm. Correspondingly, the sensor with the NIP receptor shows almost no change in $\boldsymbol{Z_{abs}}$.

3.5 Selectivity

300 ppm stock solutions of histamine, spermine, spermidine, and putrescine each were prepared in 1X PBS (ionic strength = 162.7 mM, pH = 7.4). These molecules are part of a family of chemicals named 'biogenic amines' and are found along histamine in seafood. The sensor

performance is then evaluated by measuring the change in $\boldsymbol{Z_{abs}}$, which is given by $\Delta Z_{abs}/Z_{abs,0} = (Z_{abs,0} - Z_{abs,300\ ppm})/Z_{abs,0;}$ where the second index of $\boldsymbol{Z_{abs}}$ represents the concentration of spiked biogenic amines. The results of the selectivity test are shown in **Figure 6**. The results show that the MIP sensor is selective to histamine.

4. Portable smartphone-based device for semi-quantitative histamine sensing

4.1 Device architecture

The device architecture for the smartphone-based device is shown in **Figure 7**. A separate unit labelled "E-card" is fabricated. The E-card contains a MCU which communicates with an AD5933 impedance analyzer. The absolute value of impedance at 4000 Hz is recorded for each sample tested. The results are communicated to the Bluetooth module. The Bluetooth module sends the data to a smartphone device. A custom-build app on the smartphone reads and analyzes the data. The concentration of histamine is displayed on the smartphone in a semi-quantitative fashion. The final results are displayed in one of three ways:

i) Histamine concentration is less than 100 ppm

ii) Histamine concentration is between 101 ppm and 300 ppm

iii) Histamine concentration is greater than 300 ppm

300 ppm is chosen as the concentration of interest as this is the maximum limit of histamine that is allowed in seafood in mainland China.

4.2 Portable device testing protocol

Since the variance is very high between devices (greater than 10% variation at 0 ppm between devices), it was determined to provide the user with 2 calibration solutions of 100 ppm

histamine and 300 ppm histamine. Then the user is prompted to select a calibration solution (for this example; the user selects 100 ppm calibration solution). Then the user tests the impedance value of the calibration solution for 5 times. Then the sensor head is cleaned in deionized water for 2 minutes. Next, the user is prompted to test with the sample solution for 5 times. If the value of impedance for the sample is greater than that for the calibration solution, the result is displayed as histamine concentration is less than 100 ppm. Otherwise, the user is prompted to recalibrate the sensor with the 300 ppm solution and the process is repeated. If $\boldsymbol{Z_{abs}}$ (at f = 4000 Hz) for the sample is less than that for the 300 ppm calibration solution, the result is displayed as histamine concentration is greater than 300 ppm, else, the result is displayed as the histamine concentration is between 100 and 300 ppm. The detailed explanation of this concept is explained in the flowchart in **Figure 8**.

4.3 Saving data

The data from the portable device test is then stored of flexible NFC sticker tags by tapping the smartphone (with the NFC function on) on the NFC tag. A video demonstration of the portable device testing the histamine concentration in a supermarket-purchased shrimp sample is shown in **Supporting Information Video S4**.

4.4 Portable device test data

The test data for the portable device is presented in Table 1.

Table 1: Evaluation of portable test device

Sample #	*Sample histamine concentration (ppm)*	*Sample matrix*	*Portable device result*	*Evaluation*
0001	500	Deionized water	Histamine > 300 ppm	**OK**
0002	0	Deionized water	Histamine < 100 ppm	**OK**

0003	200	1 × PBS	101 ppm < Histamine < 300 ppm	**OK**
0004	600	Deionized water	Histamine > 300 ppm	**OK**
0006	100	1 × PBS	101 ppm < Histamine < 300 ppm	**Acceptable**
0007	600	1 × PBS	Histamine > 300 ppm	**OK**

As shown in **Table 1**, the portable smartphone-based device results agree with the amount of histamine spiked into the sample in 6 out of 6 tests. This is a very promising result and therefore the semi-quantitative histamine analysis performed by the portable smartphone-based is deemed to be valid.

4.5 Real seafood sample test

4 samples of seafood were purchased from a local supermarket. 2 samples of *Grass Carp* (FISH A, FISH B) and 2 samples of *White Shrimp* (SHRIMP A, SHRIMP B). The 'A' samples were stored in a fumehood at 25°C to induce spoilage, before testing with portable histamine sensor and HPLC-MS. On the other hand, the 'B' samples were tested immediately after purchase. The seafood samples are shown in **Figure S3**.

Table 2: Real seafood sample test

Sample name	***Spoilage conditions***	***Portable device result***	***HPLC-MS result (ppm)***	***Evaluation***
FISH A	48 h in fumehood at 25°C	Histamine > 300 ppm	927.56	**OK**
FISH B	None	Histamine < 100 ppm	61.65	**OK**
SHRIMP A	48 h in fumehood at 25°C	Histamine > 300 ppm	1222.47	**OK**
SHRIMP B	None	Histamine < 100 ppm	33.96	**OK**

As shown in **Table 2**, the portable smartphone-based device results agree with the amount of histamine in seafood samples 4 out of 4 tests.

5. Conclusion

In this paper, we show the fabrication of a flexible histamine sensor. This device can accurately detect the presence of histamine while discriminating DL-histidine and other common

biogenic amines (spermine, spermidine and putrescine) in the range relevant exposure limits set by regulatory authorities. Finally, we showed the on-site applicability of this device by constructing a portable prototype device that can be controlled via bluetooth from a smartphone app. We believe that the flexible histamine sensor along with the portable prototype device checks all the boxes required for a robust field sensing system (required LDLs, high sensitivity, non-fragility, modularity, size and easy operability). Our ultimate goal is to have a handheld and fully quantitative device with easy operation. To achieve this, further research and product development is required in the enhancement of sensitivity and reduction of device variance via electrode design refinement, additional transduction layers and automation of testing procedures.

Acknowledgements

We would like to acknowledge Mr. Daniel Yau for technical support. This work was supported by the Research Grant Council of HKSAR Project (No. 8770006 & C7045-14E).

Received: ((will be filled in by the editorial staff))
Revised: ((will be filled in by the editorial staff))
Published online: ((will be filled in by the editorial staff))

References

Abraham, M. J., Murtola, T., Schulz, R., Páll, S., Smith, J. C., Hess, B., Lindahl, E., 2015. GROMACS: High performance molecular simulations through multi-level parallelism from laptops to supercomputers. SoftwareX. 1-2, 19-25. https://doi.org/10.1016/j.softx.2015.06.001.

Akhoundian, M., Rüter, A., Shinde, S., 2017. Ultratrace Detection of Histamine Using a Molecularly-Imprinted Polymer-Based Voltammetric Sensor. Sensors. 17, 645. http://dx.doi.org/10.3390/s17030645.

Bao, L., Sun, D., Tachikawa, H., Davidson, V. L., 2002. Improved Sensitivity of a Histamine Sensor Using an Engineered Methylamine Dehydrogenase. Anal. Chem. 74, 1144-1148. https://doi.org/10.1021/ac0106086.

Basozabal, I., Guerreiro, A., Gomez-Caballero, A., Aranzazu Goicolea, M., Barrio, R. J., 2014. Direct potentiometric quantification of histamine using solid-phase imprinted nanoparticles as recognition elements. Biosens. Bioelectron. 58, 138-144. https://doi.org/10.1016/j.bios.2014.02.054.

Bedia Erim, F., 2013. Recent analytical approaches to the analysis of biogenic amines in food samples. Trends Anal. Chem. 52, 239-247. https://doi.org/10.1016/j.trac.2013.05.018.

Belon, P., Cumps, J., Ennis, M., Mannaioni, P. F., Roberfroid, M., Sainte-Laudy, J., Wiegant, F. A. C., 2004. Histamine dilutions modulate basophil activation. Inflamm. Res. 53, 181-188. https://doi.org/10.1007/s00011-003-1242-0.

Bi, J., Tian, C., Zhang, G.-L., Hao, H., Hou, H.-M., 2020. Detection of histamine based on gold nanoparticles with dual sensor system of colorimetric and fluorescence. Foods. 9, 316. https://doi.org/10.3390/foods9030316.

Bongaers, E., Alenus, J., Horemans, F., Weustenraed, A., Lutsen, L., Vanderzande, D., Cleij, T. J., Troost, F. J., Brummer, R.-J., Wagner, P., 2010. A MIP-based biomimetic sensor for the impedimetric detection of histamine in different pH environments. Phys. Status Solidi A. 207, 837-843. https://doi.org/10.1002/pssa.200983307.

Busto, O., Valero, Y., Guasch, J., Borrull, F., 1994. Solid phase extraction applied to the determination of biogenic amines in wines by HPLC. Chromatographia. 38, 571-578. https://doi.org/10.1007/BF02277156.

Chen, L., Wang, X., Lu, W., Wu, X., Li, J., 2016. Molecular imprinting: perspectives and applications. Chem. Soc. Rev. 45, 2137-2211. https://doi.org/10.1039/c6cs00362a

Commission Regulation (EC) No 1441/2007 of 5 December 2007 amending Regulation (EC) No 2073/2005 on microbiological criteria for foodstuffs. Pages 12-29 in Official Journal of the European Union. Vol. 332. https://eur-lex.europa.eu/LexUriServ/LexUriServ.do?uri=OJ:L:2007:322:0012:0029:EN:PDF. (accessed: 27 October 2020).

Dang, A., Pesek, J. J., Matyska, M. T., 2013. The use of aqueous normal phase chromatography as an analytical tool for food analysis: Determination of histamine as a model system. Food Chem. 141, 4226-4230. https://doi.org/10.1016/j.foodchem.2013.06.005.

Delle, L. E., Huck, C., Bäcker, M., Müller, F., Grandthyll, S., Jacobs, K., Lilischkis, R., Vu, X. T., Schöning, M. J., Wagner, P., Thoelen, R., Weil, M., Ingebrandt, S., 2015. Impedimetric immunosensor for the detection of histamine based on reduced graphene oxide. Phys. Status Solidi A. 212, 1327-1334. https://doi.org/10.1002/pssa.201431863.

Delves, P. J., Roitt, I. M., 2000. The Immune System. N. Engl. J. Med. 343, 37-49. https://doi.org/10.1056/nejm200007063430107.

Eitenmiller, R. R., Wallis, J. W., Orr, J. H., Phillips, R. D., 1981. Production of Histidine Decarboxylase and Histamine by Proteus morganii. J. Food Prot. 44, 815-820. https://doi.org/10.4315/0362-028x-44.11.815.

Hallgren, J., Gurish, M. F., 2014. Granule maturation in mast cells: Histamine in control. Eur. J. Immunol. 44, 33-36. https://doi.org/10.1002/eji.201344262.

Hasanzadeh, M., Shadjou, N., de la Guardia, M., 2017. Aptamer-based assay of biomolecules: Recent advances in electro-analytical approach. Trends Anal. Chem. 89, 119-132. https://doi.org/10.1016/j.trac.2017.02.003.

Henao-Escobar, W., del Torno-de Román, L., Domínguez-Renedo, O., Alonso-Lomillo, M. A., Arcos-Martínez, M. J., 2016. Dual enzymatic biosensor for simultaneous amperometric determination of histamine and putrescine. Food Chem. 190, 818-823. https://doi.org/10.1016/j.foodchem.2015.06.035.

Henao-Escobar, W., Domínguez-Renedo, O., Alonso-Lomillo, M. A., Arcos-Martínez, M. J., 2015. Resolution of quaternary mixtures of cadaverine, histamine, putrescine and tyramine by the square wave voltammetry and partial least squares method. Talanta. 143, 97-100. https://doi.org/10.1016/j.talanta.2015.05.047.

Horemans, F., Alenus, J., Bongaers, E., Weustenraed, A., Thoelen, R., Duchateau, J., Lutsen, L., Vanderzande, D., Wagner, P., Cleij, T. J., 2010. MIP-based sensor platforms for the detection of histamine in the nano- and micromolar range in aqueous media. Sens. Actuators B Chem. 148, 392-398. https://doi.org/10.1016/j.snb.2010.05.003.

Huang, W., Lin, Z., van Gunsteren, W. F., 2011. Validation of the GROMOS 54A7 Force Field with Respect to β-Peptide Folding. J. Chem. Theory Comput. 7, 1237-1243. https://doi.org/10.1021/ct100747y.

Ijomah, P., Clifford, M. N., Walker, R., Wright, J., Hardy, R., Murray, C. K., 1991. The importance of endogenous histamine relative to dietary histamine in the aetiology of scombrotoxicosis. Food Addit. Contam. 8, 531-542. https://doi.org/10.1080/02652039109374005.

Johnson, A. R., Erdös, E. G., 1973. Release of Histamine from Mast Cells by Vasoactive Peptides. Proc. Soc. Exp. Biol. Med. 142, 1252-1256. https://doi.org/10.3181/00379727-142-37219.

Jutel, M., Blaser, K., Akdis, C., 2005. Histamine in chronic allergic responses. J. Invest. Allergol. Clin. Immunol. 15, 1-8. https://doi.org/10.1159/000085108.

Köse, S., Kaklıkkaya, N., Koral, S., Tufan, B., Buruk, K. C., Aydın, F., 2011. Commercial test kits and the determination of histamine in traditional (ethnic) fish products-evaluation against an EU accepted HPLC method. Food Chem. 125, 1490-1497. https://doi.org/10.1016/j.foodchem.2010.10.069.

Kumar, N., Goyal, R. N., 2018. Silver nanoparticles decorated graphene nanoribbon modified pyrolytic graphite sensor for determination of histamine. Sens. Actuators B Chem. 268, 383-391. https://doi.org/10.1016/j.snb.2018.04.136.

Liu, C.-X., Zhao, J., Zhang, R.-R., Zhang, Z.-M., Xu, J.-J., Sun, A.-L., Chen, J., Shi, X.-Z., 2020. Development and application of fluorescence sensor and test strip based on molecularly imprinted quantum dots for the selective and sensitive detection of propanil in fish and seawater samples. J. Hazard. Mater. 389, 121884. https://doi.org/10.1016/j.jhazmat.2019.121884.

Liu, S.-J., Xu, J.-J., Ma, C.-L., Guo, C.-F., 2018. A comparative analysis of derivatization strategies for the determination of biogenic amines in sausage and cheese by HPLC. Food Chem. 266, 275-283. https://doi.org/10.1016/j.foodchem.2018.06.001.

406 Lv, R., Huang, X., Dai, C., Ye, W., Tian, X., 2019. A rapid colorimetric sensing unit for
407 histamine content of mackerel using azo reagent. J. Food Process Eng. 42, e13099.
408 https://doi.org/10.1111/jfpe.13099.
409 Maintz, L., Novak, N., 2007. Histamine and histamine intolerance. Am. J. Clin. Nutr. 85, 1185-
410 1196. https://doi.org/10.1093/ajcn/85.5.1185.
411 Malde, A. K., Zuo, L., Breeze, M., Stroet, M., Poger, D., Nair, P. C., Oostenbrink, C., Mark, A.
412 E., 2011. An Automated Force Field Topology Builder (ATB) and Repository: Version 1.0. J.
413 Chem. Theory Comput. 7, 4026-4037. https://doi.org/10.1021/ct200196m.
414 Marcobal, A., Polo, M. C., Martín-Álvarez, P. J., Moreno-Arribas, M. V., 2005. Biogenic amine
415 content of red Spanish wines: comparison of a direct ELISA and an HPLC method for the
416 determination of histamine in wines. Food Res. Int. 38, 387-394.
417 https://doi.org/10.1016/j.foodres.2004.10.008.
418 Martínez, L., Andrade, R., Birgin, E. G., Martínez, J. M., 2009. PACKMOL: A package for
419 building initial configurations for molecular dynamics simulations. J. Comput. Chem. 30, 2157-
420 2164. https://doi.org/10.1002/jcc.21224.
421 Minamiki, T., Minami, T., Yokoyama, D., Fukuda, K., Kumaki, D., Tokito, S., 2015. Extended-
422 gate organic field-effect transistor for the detection of histamine in water. Jpn. J. Appl. Phys. 54,
423 04DK02. https://doi.org/10.7567/jjap.54.04dk02.
424 Mohammed, G. I., Bashammakh, A. S., Alsibaai, A. A., Alwael, H., El-Shahawi, M. S., 2016. A
425 critical overview on the chemistry, clean-up and recent advances in analysis of biogenic amines
426 in foodstuffs. Trends Anal. Chem. 78, 84-94. https://doi.org/10.1016/j.trac.2016.02.007.
427 Önal, A., 2007. A review: Current analytical methods for the determination of biogenic amines
428 in foods. Food Chem. 103, 1475-1486. https://doi.org/10.1016/j.foodchem.2006.08.028.

Papageorgiou, M., Lambropoulou, D., Morrison, C., Kłodzińska, E., Namieśnik, J., Płotka-Wasylka, J., 2018. Literature update of analytical methods for biogenic amines determination in food and beverages. Trends Anal. Chem. 98, 128-142. https://doi.org/10.1016/j.trac.2017.11.001.

Qi, J., Li, B., Zhou, N., Wang, X., Deng, D., Luo, L., Chen, L., 2019. The strategy of antibody-free biomarker analysis by in-situ synthesized molecularly imprinted polymers on movable valve paper-based device. Biosens. Bioelectron. 142, 111533. https://doi.org/10.1016/j.bios.2019.111533.

Rotariu, L., Lagarde, F., Jaffrezic-Renault, N., Bala, C., 2016. Electrochemical biosensors for fast detection of food contaminants – trends and perspective. Trends Anal. Chem. 79, 80-87. https://doi.org/10.1016/j.trac.2015.12.017.

Schirone, M., Visciano, P., Tofalo, R., Suzzi, G., 2017. Histamine Food Poisoning. in: Hattori, Y. and Seifert, R., Histamine and Histamine Receptors in Health and Disease. Springer International Publishing, Cham, pp.217-235.

Shi, R., Feng, S., Park, C. Y., Park, K. Y., Song, J., Park, J. P., Chun, H. S., Park, T. J., 2020. Fluorescence detection of histamine based on specific binding bioreceptors and carbon quantum dots. Biosens. Bioelectron. 167, 112519. https://doi.org/10.1016/j.bios.2020.112519.

Staruskiewicz, W. F., Jr., 1977. AOAC Official Method of Analysis. 977.13 Histamine in Seafood Fluorometric Method, First Action 1977, Final Action 1987, Fish and Other Marine Products. AOAC Official Method of Analysis (1995) Supplement. 16-18. https://members.aoac.org/AOAC_Docs/OMA/977_13aoacmethod.pdf. (accessed: 27 October 2020)

Stein, M., Schiavi, R., Camerino, M., 1976. Influence of brain and behavior on the immune system. Science. 191, 435-440. https://doi.org/10.1126/science.1108202.

Tahmouzi, S., Khaksar, R., Ghasemlou, M., 2011. Development and validation of an HPLC-FLD method for rapid determination of histamine in skipjack tuna fish (Katsuwonus pelamis). Food Chem. 126, 756-761. https://doi.org/10.1016/j.foodchem.2010.11.060.

Tang, T., Qian, K., Shi, T., Wang, F., Li, J., Cao, Y., Hu, Q., 2011. Monitoring the contents of biogenic amines in sufu by HPLC with SPE and pre-column derivatization. Food Control. 22, 1203-1208. https://doi.org/10.1016/j.foodcont.2011.01.018.

Taylor, S. L., 1985. Histamine poisoning associated with fish, cheese, and other foods. World Health Organization, Geneva.

Titantah, J. T., Karttunen, M., 2013. Water dynamics: Relation between hydrogen bond bifurcations, molecular jumps, local density & hydrophobicity. Sci. Rep. 3, 2991. https://doi.org/10.1038/srep02991.

Trikka, F. A., Yoshimatsu, K., Ye, L., Kyriakidis, D. A., 2012. Molecularly imprinted polymers for histamine recognition in aqueous environment. Amino Acids. 43, 2113-2124. https://doi.org/10.1007/s00726-012-1297-8.

Wang, H., Da, L., Yang, L., Chu, S., Yang, F., Yu, S., Jiang, C., 2020. Colorimetric fluorescent paper strip with smartphone platform for quantitative detection of cadmium ions in real samples. J. Hazard. Mater. 392, 122506. https://doi.org/10.1016/j.jhazmat.2020.122506.

Yoshikawa, M., Tharpa, K., Dima, Ş.-O., 2016. Molecularly Imprinted Membranes: Past, Present, and Future. Chem. Rev. 116, 11500-11528. https://doi.org/10.1021/acs.chemrev.6b00098.

Zeng, K., Tachikawa, H., Zhu, Z., Davidson, V. L., 2000. Amperometric Detection of Histamine with a Methylamine Dehydrogenase Polypyrrole-Based Sensor. Anal. Chem. 72, 2211-2215. https://doi.org/10.1021/ac9911138.

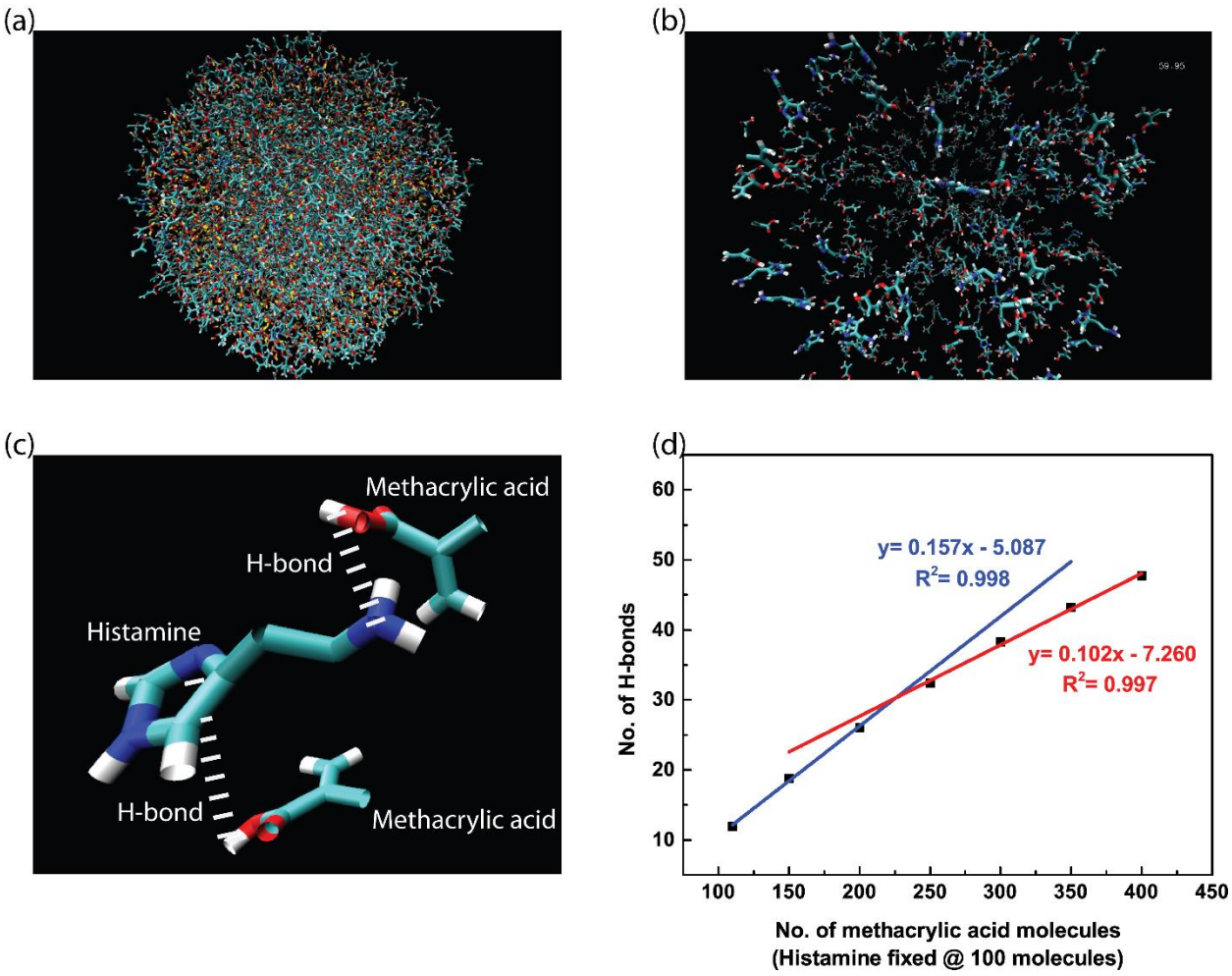

475

476 **Figure 1.** Computer simulation results **(a)** GROMACS model screenshot extracted from visual
477 molecular dynamics (VMD) tool showing the entire system consisting of methacrylic acid,
478 histamine, porogen solvent (DMSO) and crosslinker (ethylene glycol dimethacrylate) **(b)**
479 GROMACS model screenshot extracted from VMD tool showing the system with only
480 methacrylic acid and histamine (solvent & crosslinker are hidden). **(c)** GROMACS model
481 screenshot extracted from VMD tool showing the close-up of histamine forming 2 hydrogen bonds
482 (H-bonds) with 2 distinct methacrylic acid molecules. **(d)** Number of hydrogen bonds (H-bonds)
483 between methacrylic acid and histamine as a function of number of acrylic acid molecules in the

model.

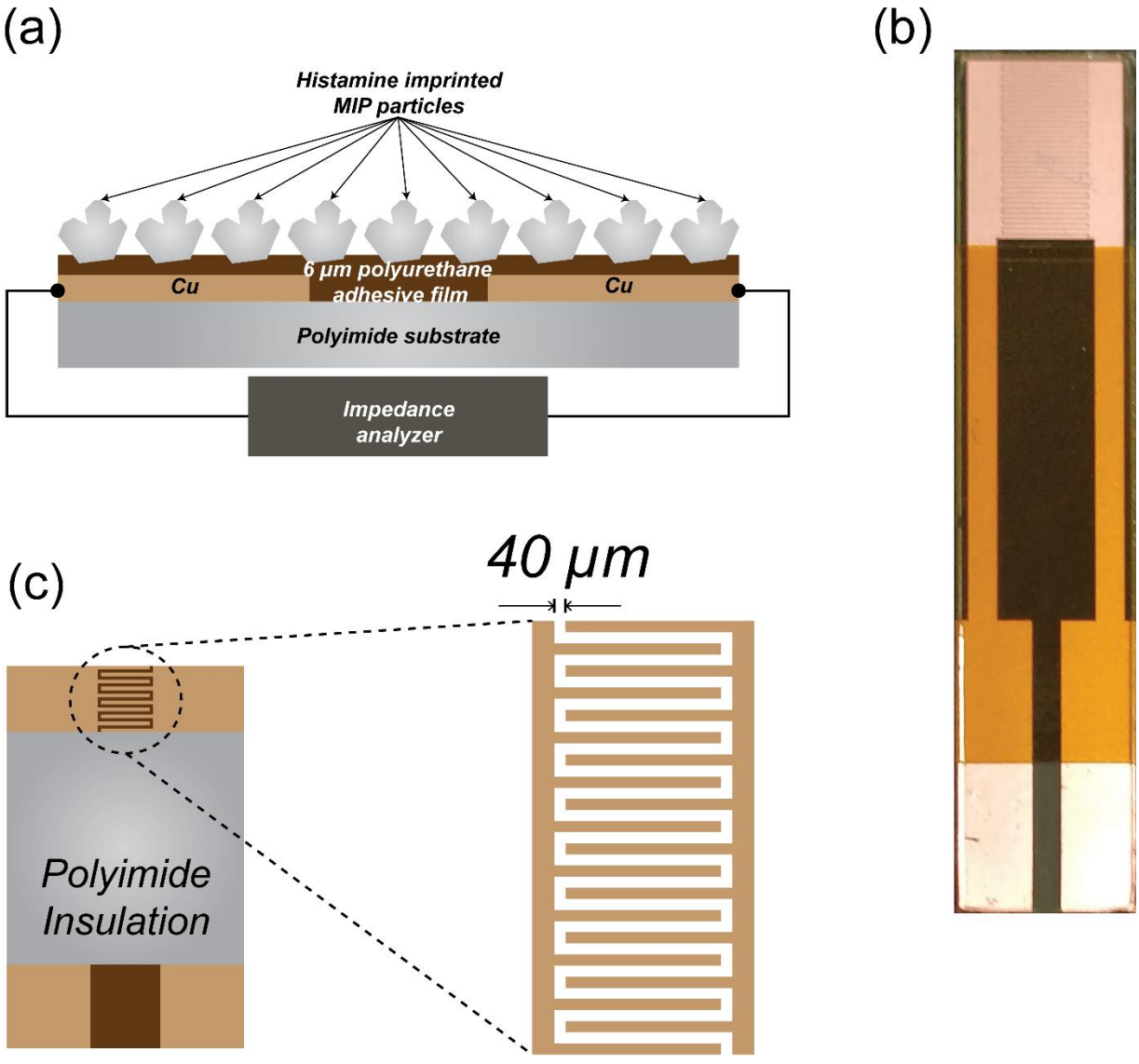

Figure 2. (a) Schematic of sensing setup for the flexible histamine sensor. **(b)** Photograph of a histamine sensor **(c)** Illustration of the interdigitated electrode pattern used in the in flexible histamine sensor.

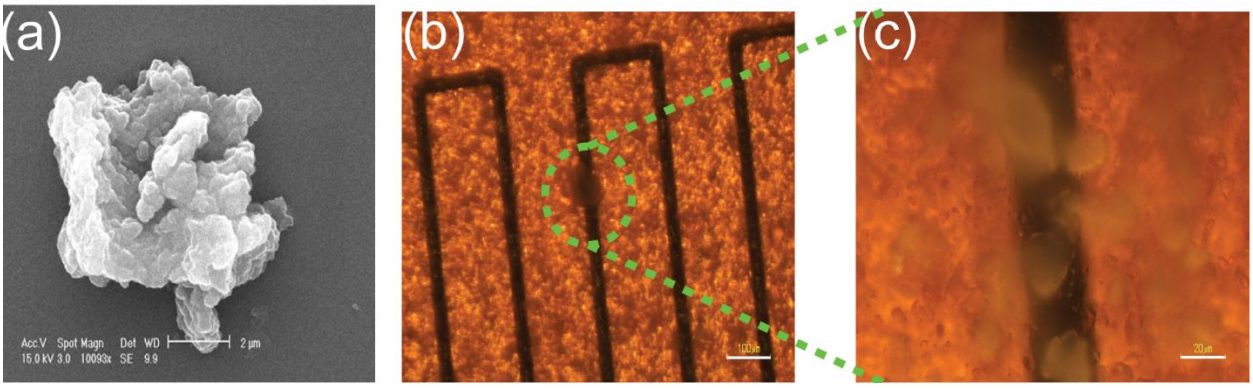

Figure 3. (a) SEM image of the MIP micro-particle (Scale bar: 2 µm) **(b)** Optical microscope image of interdigitated electrode (Scale bar: 100 µm). **(c)** Optical microscopy image of the channel between interdigitated electrode (Scale bar: 20 µm).

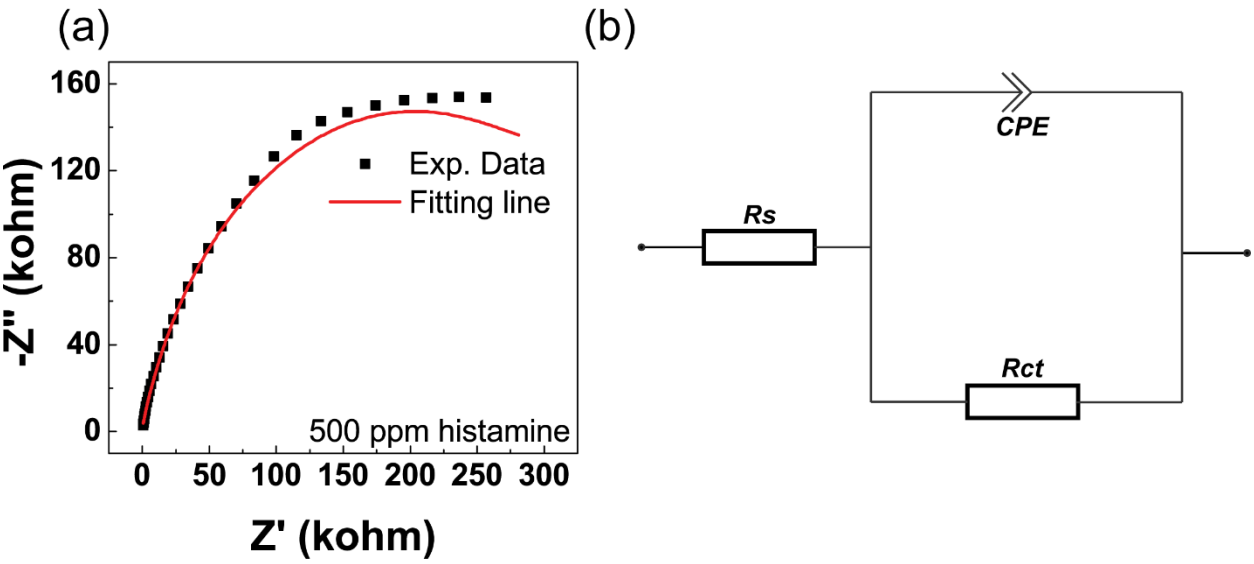

Figure 4. (a) Nyquist plot showing the good fit between experimental data (500 ppm histamine in DI water) and equivalent circuit model. **(b)** Schematic of equivalent circuit which is used to model the impedance behavior.

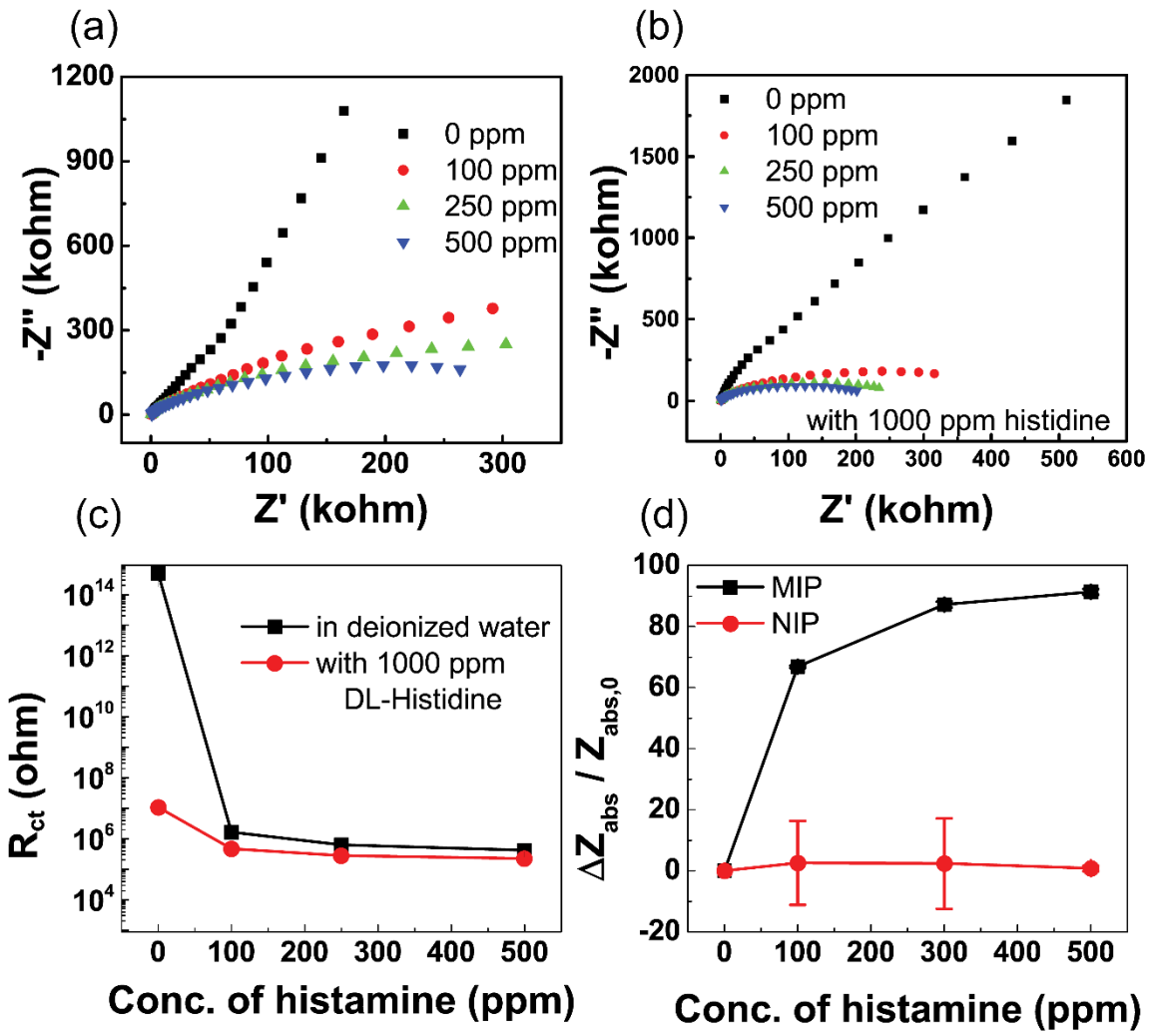

497

498 **Figure 5.** Nyquist plots of impedance response with varying concentration of histamine diluted
499 **(a)** in deionized water **(b)** in 1000 ppm histidine. **(c)** Calibration curve of histamine in 2
500 background solutions namely: deionized water and 1000 ppm DL-histidine, using extracted charge
501 transfer resistance values. **(d)** Calibration curve of histamine with MIP and corresponding NIP
502 receptors using Z_{abs} value at 4000 Hz.

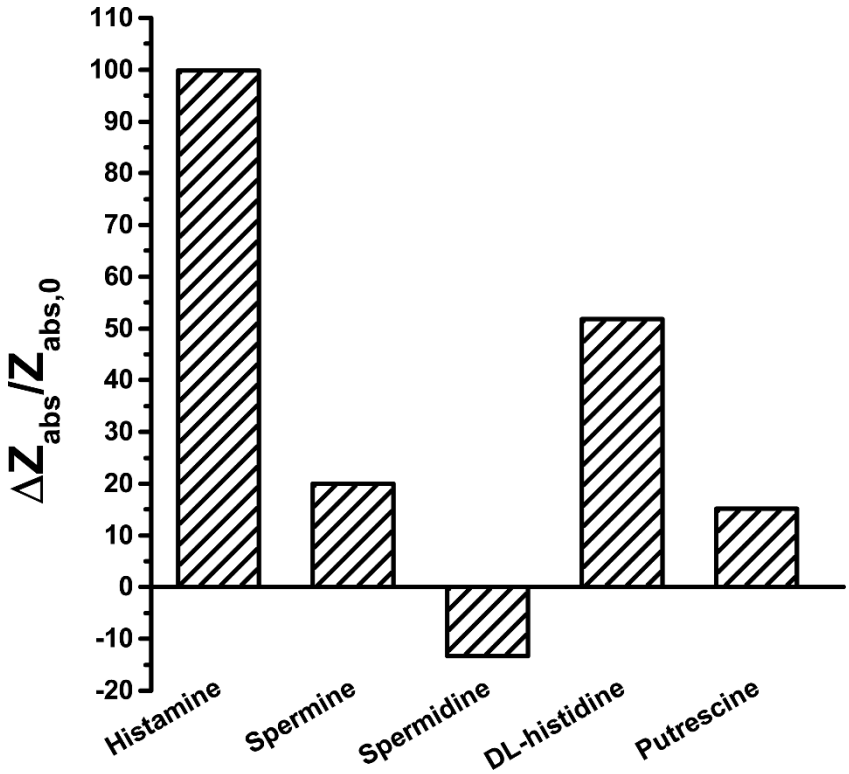

503

504 **Figure 6.** Selectivity performance of the portable device for histamine sensing. Concentration of

505 each solution is 300 ppm.

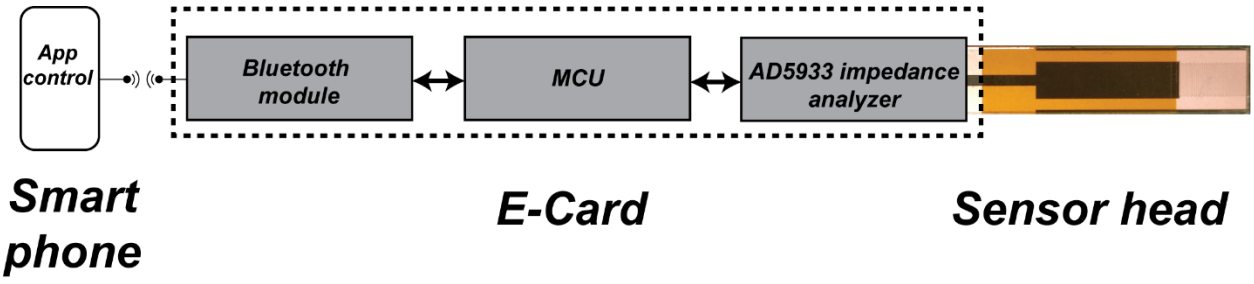

506

507 **Figure 7.** Schematic figure showing the internal workings of the smartphone based portable device

508 for histamine sensing.

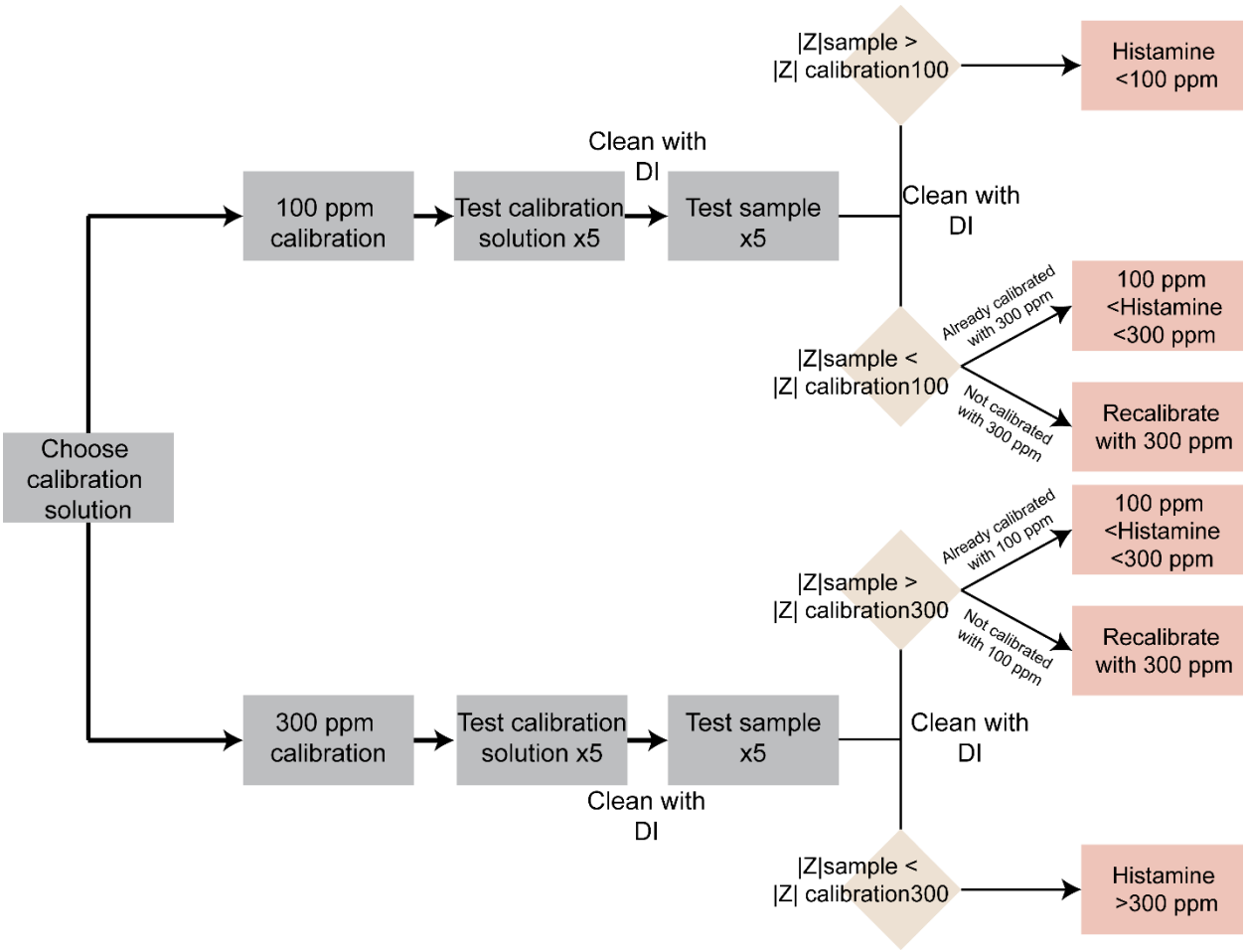

509

510 **Figure 8.** Flowchart showing the testing protocol for the smartphone-based portable device

511